Vortex shedding and aerodynamic forces on a circular cylinder in linear shear flow at subcritical Reynolds number

S. Cao[a],*, S. Ozono[b], K. Hirano[b], Y. Tamura[a]

[a]*Wind Engineering Research Center, Tokyo Polytechnic University, 1583 Iiyama, Atsugi, Kanagawa 243-0297, Japan*
[b]*Faculty of Engineering, Miyazaki University, Miyazaki 889-2192, Japan*

Abstract

Vortex shedding and aerodynamic forces on a circular cylinder in a linear shear flow with its axis normal to the plane of the velocity shear profile at subcritical Reynolds number are investigated experimentally. The shear parameter β, which is based on the velocity gradient, cylinder diameter and upstream mean velocity at the center plane of the cylinder, varies from 0 to 0.27. The Strouhal number has no significant variation with the shear parameter. The time-mean base pressure increases and the fluctuating component of the base pressure decreases significantly with increasing shear parameter. Vortex shedding is suppressed by the velocity shear. Dislocation of the stagnation point takes place and this influences the pressure distribution around the cylinder together with the velocity shear. A mean lift force arises in the shear flow due to asymmetry of the pressure distribution, and it acts from the high velocity side to the low velocity side. In addition, the lift coefficient increases and the drag coefficient decreases with increasing shear parameter.
© 2007 Elsevier Ltd. All rights reserved.

Keywords: Aerodynamic force; Base pressure; Cylinder; Shear parameter; Strouhal number; Vortex shedding

1. Introduction

The majority of studies on unsteady flow past a circular cylinder have been conducted under symmetric approaching flow conditions in which equal strength vortices are alternately shed from each side of the body. However, in practice, the approaching flow very often has some asymmetry. Therefore, it is of great interest to investigate the basic roles that asymmetry plays in vortex shedding behavior. Recently, Ozono et al. (1997, 1999) examined vortex shedding from a cylinder with some asymmetrical conditions, e.g. in a stably stratified flow or with a short splitter plate placed in the wake asymmetrically. They found that asymmetry plays a role in suppressing vortex shedding and accordingly reducing vortex-induced aerodynamic force. In this study, we investigate the effects of velocity shear, a kind of asymmetry of the oncoming flow, on vortex shedding from a circular cylinder with its axis normal to the plane of the velocity shear profile. The shear parameter is defined as $\beta = G(D/U_c) = (\mathrm{d}U/\mathrm{d}y)(D/U_c)$, where U_c is the mean velocity at the center plane, D is the diameter of the circular cylinder and G is the velocity gradient. The main motivation of this research is to realize how the vortex shedding behavior and the aerodynamic force change with increase of this parameter.

---

*Corresponding author. Tel.: +81 46 242 9656; fax: +81 46 242 9656.
E-mail address: cao@arch.t-kougei.ac.jp (S. Cao).

The aerodynamics of a bluff body in shear flow have been widely investigated in civil engineering field, where the structures are immersed in a planetary boundary layer with a velocity shear [for example, Woo et al. (1989)]. However, in these researches, bluff body models were placed parallel to the plane of velocity shear, which is different from present study. There are many situations in which a bluff body is placed normal to the plane of velocity shear, for instance, bridge decks in an atmospheric boundary layer. Since special meteorological phenomena, terrain effects and so on, can produce strong local shear flows, the variation of vortex shedding and aerodynamic forces with the shear parameter need to be studied in detail.

There have been several reported experimental studies on shear effects, however the disagreement in the results was significant. Kiya et al. (1980) investigated vortex shedding from a cylinder in moderate Reynolds number shear flows (Re = 35–1500) in a water tank. They found that the critical Reynolds number for vortex shedding to take place is higher in shear flow than in uniform flow. They also found that the Strouhal number decreases slightly with β when β is small, and then increases obviously with β at large β. Kwon et al. (1992) reported similar results for $0.05 < \beta < 0.25$ at Re = 35–1600. However, Reynolds number dependency is significant in these Reynolds number ranges, so that study at high Reynolds number is required for practical engineering problems. For the aerodynamic forces acting on cylinders, Adachi and Kato (1975) investigated the flow around a cylinder with β varied from 0 to 0.04 at Re = 2.67×10^3–1.07×10^4. They reported that both mean drag and lift force increase with β, and the lift force acts from the high velocity side to low velocity side. Hayashi and Yoshino (1990) investigated experimentally the aerodynamic force experienced by a circular cylinder in shear flow ($\beta = 0.15$) at Re = 6×10^4 and found that drag decreases in shear flow and the lift force acts from the high velocity side to the low velocity side. Meanwhile, numerical results obtained by Tamura et al. (1980) at Re = 40 and 80 showed that the lift force acts from the low velocity side to the high velocity side. Recently, Sumner and Akosile (2003) investigated intensively the flow and aerodynamic force of a circular cylinder at Re = 4.0×10^4–9.0×10^4 within a low shear parameter range of $\beta = 0.02$–0.07 and arrived at similar conclusions as Kwon et al. (1992) and Hayashi and Yoshino (1990). Cao et al. (2000) investigated vortex shedding of a circular cylinder in strong shear flow at subcritical Reynolds number. However, the variations of vortex shedding and aerodynamic forces with shear parameter and the mechanisms that lead to these variations are not fully understood. In this study, we reproduced over 20 kinds of shear flow with a large velocity shear range of $0 < \beta < 0.27$, with the aid of actively-controlled multiple-fan wind tunnels. The flow field as well as the pressure distribution around cylinders were measured in order to investigate the shear effects at Re = 1.0×10^4–5.5×10^4.

Experiments were carried out in multiple-fan wind tunnels, a small one with 11 fans (hereafter called wind tunnel A) and a large one with 99 fans (hereafter called wind tunnel B), in Miyazaki University, Japan (Cao et al., 2001). All the fans were controlled individually by one computer. The main objective of this study was to clarify the shear effects on the vortex shedding and aerodynamic forces on circular cylinders. The variations of Strouhal number, mean and fluctuating base pressures with shear parameter were examined to study the vortex shedding behavior. The mean pressure distributions around a circular cylinder in shear flows were also investigated. Individual contributions of dislocation of stagnation point and velocity shear on the pressure distribution are discussed. Variations of drag and lift forces acting on the circular cylinders with shear parameter, and the physical mechanism for these variations are presented.

2. Experimental set-up

The shear parameter β was used to express the extent of velocity shear. Fig. 1 shows a schematic of the shear flow configuration. The origin of the coordinate system is the center of the circular cylinder. The magnitude of the shear parameter implies the velocity difference between the top and bottom of the cylinder, i.e., $\beta = 0.2$ means $U_A - U_B = 0.2 U_c$. An increase in velocity gradient G or cylinder diameter D, or a decrease in velocity U_c, results in an increase in shear parameter. In order to obtain a large shear parameter at a high Reynolds number, three smooth circular cylinders of different diameters, $D = 50$, 90 and 110 mm were utilized, although the blockage ratio was large and the aspect ratio was relatively small for the large models. The blockage and aspect ratios for all the models are summarized in Table 1 (shown later). The aerodynamic forces obtained in this study are influenced by combined effects of blockage and aspect ratios. The commonly used methods, for instance Maskell's (1963) method, cannot be applied to correct the blockage effect in this study. Therefore, we did not correct the effects of blockage and aspect ratios. Instead, we changed the shear parameter for each model and clarified the shear effects according to the results obtained. Comparisons among the models were not conducted. The Reynolds number based on diameter D and velocity at center plane U_c was between 1.0×10^4 and 5.5×10^4. It is noteworthy that the velocity U_c ($U_c = 5$ m/s) at the center plane was kept constant when we changed the velocity shear for each circular cylinder model. That is to say, the Reynolds number was maintained for each model.
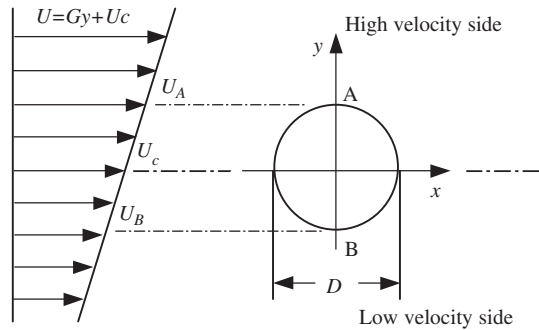
Fig. 1. Schematic of shear flow configuration.

Table 1
Summary of experimental models and St, $\bar{C}_{pb}$, C'_{pb} at uniform flow

Diameter of the model (mm)	50	90	110
Wind tunnel	Tunnel A	Tunnel A	Tunnel B
Blockage ratio (BR) (%)	5.0	9.0	6.1
Aspect ratio (AR)	4	2.22	8
Reynolds number	1.7×10^4	3.0×10^4	3.6×10^4
St	0.19	0.20	0.19
$\bar{C}_{pb}$	−1.0	−1.3	−1.5
C'_{pb}	0.13	0.21	Not measured

The experiments were conducted in a 0.2 m wide, 1.0 m high and 3.3 m long test-section of wind tunnel A, and a 2.6 m wide, 1.8 m high and 15.5 m test-section of wind tunnel B. Two-dimensional flow was maintained in both test-sections. The available maximum velocity gradient was $14.8\,\text{s}^{-1}$ in wind tunnel A and $5.8\,\text{s}^{-1}$ in wind tunnel B. Accordingly, the shear parameter range was 0–0.27 and 0–0.12 in these two wind tunnels, respectively. Vortex shedding behavior was mainly investigated in wind tunnel A because a larger velocity gradient could be obtained, although the aspect ratio effect could not to be ignored. The time-mean base pressure, fluctuating component of base pressure and the velocity field in the wake were measured. Wind tunnel B was utilized to measure the pressure distribution around a circular cylinder and to qualitatively confirm the results obtained in wind tunnel A. 72 pressure tappings were provided around the cylinder at angle increments of 5°. Circular cylinder models were placed directly between the wind tunnel side walls in wind tunnel A, while square end-plates with dimensions of $8D \times 8D$ were provided to the model to maintain two dimensionality of flow in wind tunnel B.

The velocity U_c at the center plane of the cylinder was used as the reference velocity to define Strouhal number and pressure coefficient. Drag and lift forces are calculated by integrating the pressure distribution around the cylinder.

3. Generated shear flows

Experiments were carried out at $2.9H$ and $5.5H$ (H: height of the test-section) downstream of the entrance of the test section in wind tunnels A and B, respectively. Sixteen kinds of shear flow ($U_c = 5\,\text{m/s}$, $G = 0$–$14.8\,\text{s}^{-1}$) were generated in wind tunnel A, and 5 kinds of shear flow ($U_c = 5\,\text{m/s}$, $G = 0$–$5.8\,\text{s}^{-1}$) were generated in wind tunnel B. Feedback of the input data of the fans was conducted to improve the linearity of the generated velocity shear in the wind tunnels (Cao et al., 2001). Fig. 2 shows examples of the velocity profiles of the generated shear and uniform flows in wind tunnel A. It can be seen that the shear flows were reproduced well. Shear flows were generated in tunnel B also with satisfactory linearity (not shown here). The velocity gradient had a small downstream decrease, less than 2% within a downstream distance of −400 to 400 mm near the turntable location when G equaled $6.6\,\text{s}^{-1}$. In addition, a very slight vertical mean velocity component was found in shear flows, which leads to a maximum flow inclination of 0.25° in the shear range of present study.
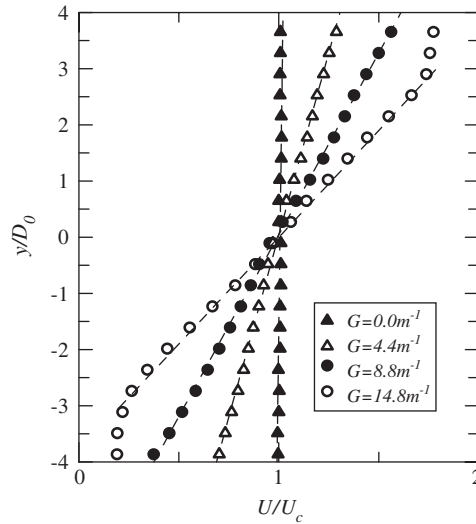
Fig. 2. Velocity profiles of generated shear flows (D_0 is the diameter of the large cylinder, $D_0 = 90$ mm).
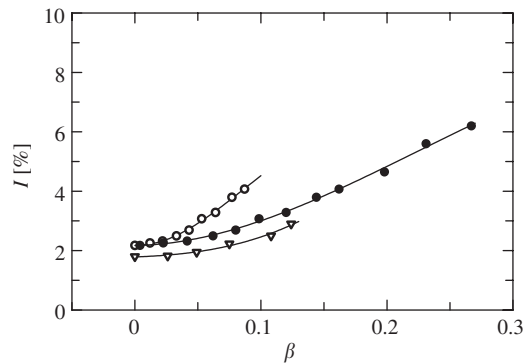

Fig. 3. Variation of velocity fluctuations with β: $\circ$, $D = 50$ mm cylinder in wind tunnel A; $\bullet$, $D = 90$ mm cylinder in wind tunnel A; $\triangledown$, $D = 110$ mm cylinder in wind tunnel B.

Turbulence inevitably occurs with the velocity shear at the present Reynolds number. Fig. 3 shows that the normalized velocity fluctuation $I = \sqrt{\overline{u'^2}}/U_c$ increases with β. Here, we note that the multiple fan wind tunnels were originally designed for modelling the turbulent boundary layer flow. It has a large turbulence intensity of about 2% in the smooth flow. It is well known that turbulence intensity significantly influences vortex shedding from a circular cylinder. The increase of turbulence intensity in a shear flow complicates the aerodynamics of the circular cylinder and requires attention with regard to the shear effects.

4. Results and discussion

4.1. Vortex shedding in uniform flow

In order to clarify the velocity shear effects on the aerodynamics of a cylinder, comparative experiments were at first carried out in uniform flow. Through the comparison with the data obtained by other researchers, the results of the present study with great, however uncorrectable, effects of aspect ratio and blockage ratio can be evaluated.

Table 1 summarizes the Strouhal number and base pressure obtained for each model, together with the blockage ratio, aspect ratio and Reynolds number. Differences in Strouhal number and base pressure due to the blockage ratio

and aspect ratio are obvious. It is known that the Strouhal number and base pressure depends greatly on the aspect ratio, blockage ratio and so on at subcritical Reynolds number. For instance, it has been reported that St = 0.19, $C_{pb} = -1.35$ when the aspect ratio was 6.0 and the blockage ratio was 9.0% at Re = 4.5×10^4 (West and Apelt, 1982). It has also been reported that St = 0.21, $C_{pb} = -1.60$ when the aspect ratio was 5.0 and the blockage ratio was 20.0% at Re = 1.1×10^5 (Sasaki and Hirano, 1978). In addition, it is recognized that base pressure is strongly dependent on aspect ratio when the aspect ratio is small (Sasaki and Hirano, 1978). Although the data of the present study deviate a little from these data, the variation tendencies of Strouhal number and base pressure with blockage ratio and aspect ratio are very similar. The results obtained in this study can thus be considered appropriate.

4.2. Vortex shedding in shear flow

Fig. 4 shows the present result of Strouhal number obtained at three cylinders with different aspect ratio and blockage ratio. The vortex shedding frequency is detected from the velocity fluctuation at $x = 1.0D$ downstream, $y = 0.5D$ upward from the cylinder center on the high velocity side. The present results shown in Fig. 4 are averaged from five experimental runs. The results of Kato and Adachi (1976), Sumner and Akosile (2003) and Tamura et al. (1981) are also shown for comparison. The same tendency that the Strouhal number is almost unchanged with shear parameter is shown for all the models of the present study, although its magnitude varies with model diameter due to blockage and aspect ratio effects. It agrees with the results of Kato and Adachi (1976) and Sumner and Akosile (2003) obtained in a low shear parameter range, but contradict the results of Tamura et al. (1981) and Kwon et al. (1992) obtained at large shear parameter and low Reynolds number. The Reynolds number difference is possibly the reason for this disagreement. From the results at several Reynolds numbers, Tamura et al. (1981) predicted that shear effects on vortex shedding frequency may be small when the Reynolds number becomes large, although the Strouhal number obviously increases with shear parameter at low Reynolds number. Sumner and Akosile (2003) also doubted the increase of Strouhal number in the subcritical Reynolds number region even at large shear parameter. The present results support their predictions. A conclusion can be drawn that the shear parameter has no significant influence on the vortex shedding frequency at subcritical Reynolds number in the shear parameter range of $\beta < 0.27$.

The velocity difference between the high velocity and low velocity sides of the cylinder increases with the shear parameter. With the increase of velocity difference, the strength and depth of the boundary layer, and then the vorticity generated in the separated shear layer, differ on the two sides. This possibly creates a difference in vortex shedding behavior or shear layer instability on the two sides. Measurement of the vortex shedding frequency at location $x/D = 1.0$ on both sides of the cylinder showed that the vortex shedding frequencies were the same (not shown here). Further measurement of the mean velocity also at $x/D = 1.0$ with a hot-wire anemometer showed that the velocity difference between the two sides of the body had been greatly adjusted. Fig. 5 compares the mean velocity profiles measured at $x/D = 1.0$ in uniform flow and shear flow. Note that only the results in the region $y/D > 0.5$ and $y/D < -0.5$, where the flow is forward and has low turbulence, are reliable because the measurements were conducted with a hot-wire anemometer. In the uniform flow, the flow accelerated symmetrically at both sides of the circular cylinder.
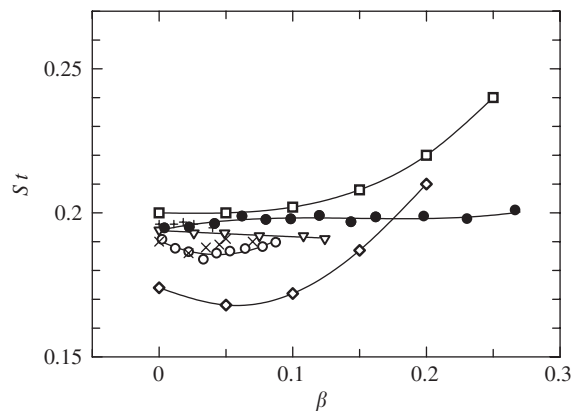

Fig. 4. Strouhal number versus shear parameter: ○, present study, AR = 4.0, BR = 5.0%, Re = 1.7×10^4; ●, present study, AR = 2.22, BR = 9.0%, Re = 3.0×10^4; ▽, present study, AR = 6.11, BR = 8.0%, Re = 3.6×10^4; ◇, Tamura et al. (1981), Re = 200; □, Tamura et al. (1981), Re = 600; ×, Sumner and Akosile (2003), Re = 4.0×10^4–9.0×10^4; +, Kato and Adachi (1976), Re = 8.0×10^3.
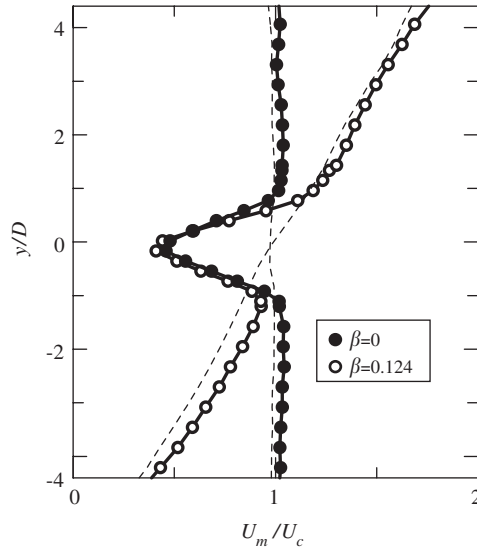
Fig. 5. Comparison of the mean velocity profile between uniform and shear flows ($D = 110$ mm, AR = 6.11, BR = 8.0%).
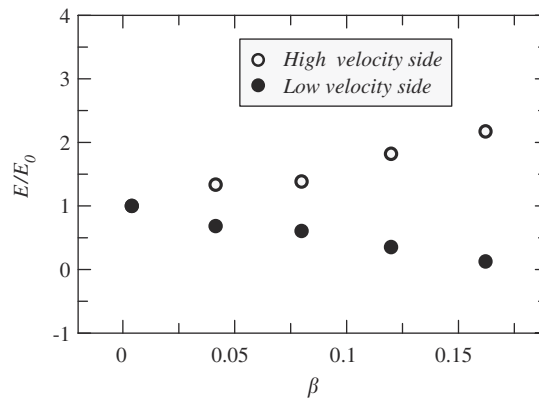

Fig. 6. Turbulence production on the high and low velocity sides at $x/D = 5.0$.

However, the flow on the low velocity side accelerated greatly compared to that on the high velocity side in the shear flow. The asymmetry in the oncoming velocity profile was greatly 'self-adjusted'. The same phenomenon was noticed for all the models with different aspect ratios and blockage ratios. Furthermore, we suggest that this acceleration on the low velocity side occurred when the flow encountered the cylinder. The pressure distribution around the cylinder shown later supports this suggestion. This phenomenon occurs due to the dislocation of the stagnation point. Discussion on this will be provided later.

Although no difference in Strouhal number can be detected immediately downstream of the cylinder, the formation of the vortex street should be different on the two sides of the cylinder, because separated vortices with opposite rotation direction on the two sides will interact with the vortex in the oncoming shear flow. Fig. 6 shows the turbulence production measured at $x/D = 5.0$, $y/D = \pm 0.5$, which is defined as $E = -\rho \overline{u'v'}(\mathrm{d}U/\mathrm{d}y)$. E is normalized in Fig. 6 by the turbulence production E_0 in the uniform flow at the same location. It can be seen that turbulence production on the high velocity side is higher than that on the low velocity side, and this difference becomes larger with increase in shear parameter. Kiya et al. (1979) predicts this phenomenon and its function in vortex street formation in his analytical study. The vortex is strengthened on the high velocity side where it has the same rotational direction with the vortex contained in the oncoming shear flow, and it is weakened on the low velocity side because its rotational direction is opposite to the vortex in the oncoming flow. We can imagine that a very complicated vortex street will be formed while it moves downstream.

Turning back to the vortex shedding behavior, Fig. 7 shows the variation of time-mean base pressure with shear parameter. The magnitude of the base pressure relates directly to the formation length of the separated vortex and is indicative of the drag experienced by the cylinder (Bearman, 1965). Fig. 7 shows that the base pressure increases with shear parameter for all the models although its magnitude varies with model diameter due to blockage and aspect ratio effects. The base pressure recovers in the shear flow. Meanwhile, Fig. 8 shows that the fluctuating component of base pressure decreases with shear parameter. The variations of base pressure imply that the vortex shedding is suppressed in the shear flow.

Instead of the vortex circulation, the magnitude of the power spectrum at the vortex shedding frequency was utilized as indicative of vortex strength (Ozono, 1999). Fig. 9 shows the variation of peak magnitude of the power spectrum of velocity fluctuation measured at $x/D = 1.0$, $y/D = 0.5$. The power spectrum decreases with shear parameter. This demonstrates vortex suppression in shear flow.

However, as discussed above, the turbulence intensity increased with velocity shear. It will require further study to distinguish the velocity shear effects from the turbulence effects. Basu (1986) reviewed several wind tunnel experimental results and concluded that the drag experienced by a cylinder increases with turbulence intensity. Therefore, it is reasonable to consider that vortex shedding is suppressed because of the velocity shear, rather than the turbulence accompanied by it. Due to the asymmetry of the oncoming flow, the separation point (shown later) and the vorticity generated in the separated shear layer is different on the two sides of the cylinder. The inequivalently separated shear layers cannot interact with each other regularly as in the non-shear situation. As a result, vortex shedding is suppressed.
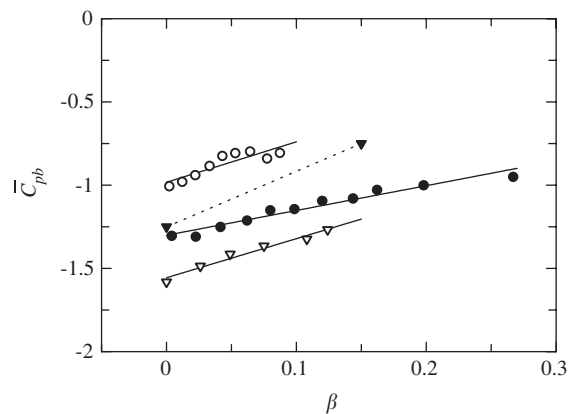

Fig. 7. Mean base pressure coefficient versus shear parameter: ▼, Hayashi et al., $Re = 6.0 \times 10^4$; other symbols, as in Fig. 4.
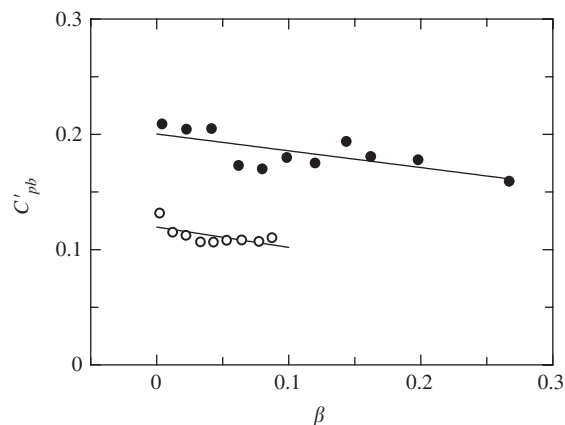

Fig. 8. Fluctuating base pressure coefficient versus shear parameter; symbols, as in Fig. 4.
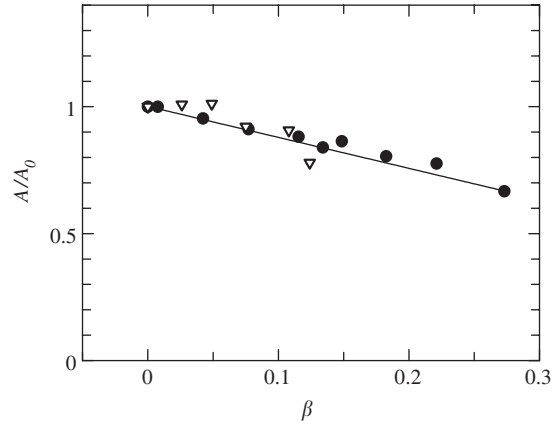
Fig. 9. Peak amplitude of power spectrum versus shear parameter; symbols, as in Fig. 4.
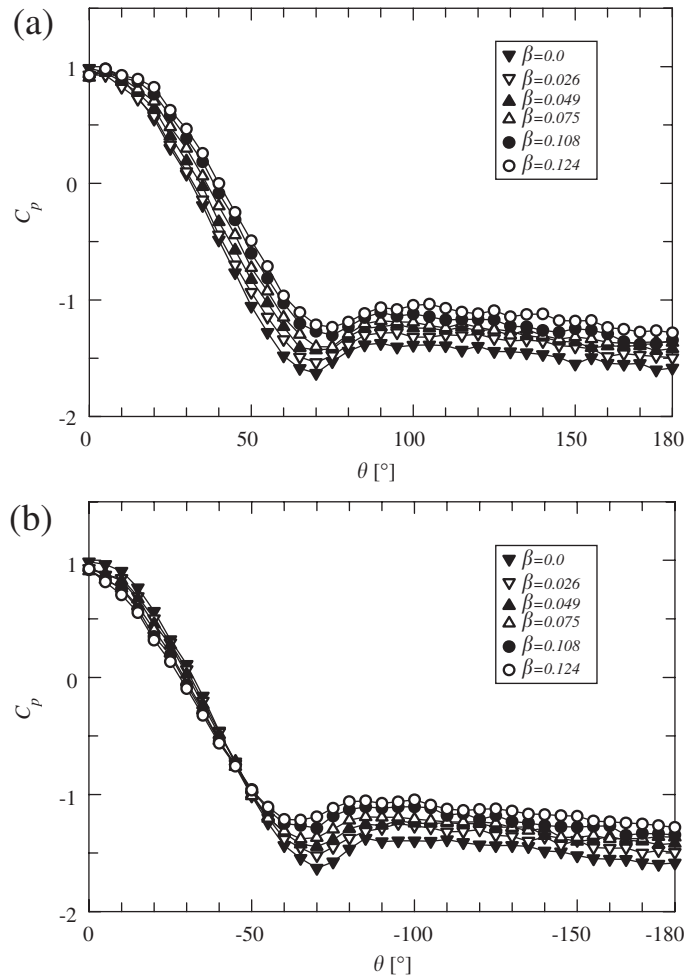

Fig. 10. Pressure distribution around a cylinder in uniform and shear flows. (a) High velocity side, (b) low velocity side.

4.3. Aerodynamic forces acting on cylinder

The pressure distribution around a cylinder was measured in uniform and shear flows at Re $= 3.64 \times 10^4$ in wind tunnel B. Mean pressure distributions on the high velocity side and the low velocity side are shown in Figs. 10(a) and (b), respectively, $\theta = 0$ is the geometrical stagnation point on the forebody; it is defined to increase to $180°$ on the high velocity side, and decrease to $-180°$ on the low velocity side. It can be seen from Fig. 10 that pressure distribution varies with shear parameter, and differs between the high velocity and low velocity sides. Base pressure recovery with increase in shear parameter can be seen. To show the shear effects on pressure distribution more clearly, the results of one kind of shear flow are compared with those of the uniform flow in Fig. 11. The pressure distribution is asymmetrical in the shear flow.

The most significant feature of the pressure distribution in the shear flow shown in Fig. 11 is that the point with the maximum pressure coefficient appears on the high velocity side, rather than at the geometrical stagnation point as in the uniform flow, and it is larger than 1.0. This is the effect of dislocation of the stagnation point, which is an essential flow feature of shear flow, as illustrated in Fig. 12 (discussed later). Looking at the pressure distribution around the cylinder, it can be seen that the pressure coefficient is larger on the high velocity side from the stagnation point to the point where the pressure is minimum. Conversely, the pressure on the low velocity side is higher from the minimum pressure point to the separation point. However, the after-body pressure is almost the same on the two sides. This can be explained by the effects of two flow features: the velocity shear and the dislocation of the stagnation point (Hayashi and Yoshino, 1990). Fig. 12 illustrates the flow around a cylinder in shear flow. The flow in front of the cylinder divides and goes to the two sides when it encounters the cylinder. Because of the dislocation of the stagnation point, which functions dominantly at the forebody of the circular cylinder, the flow becomes easier to accelerate on the low velocity side. This leads to low
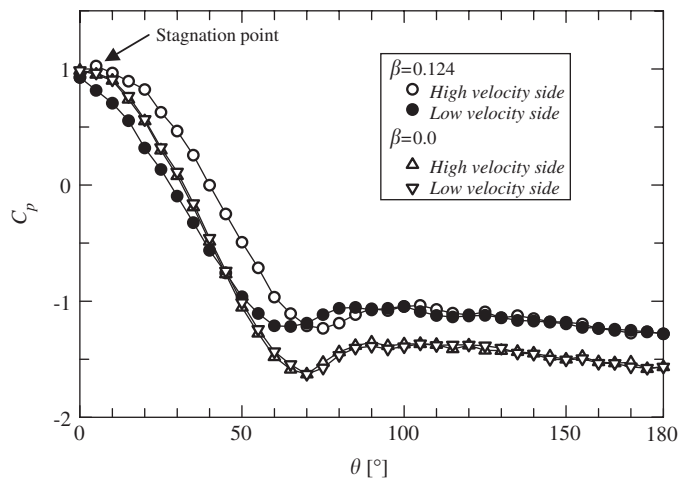

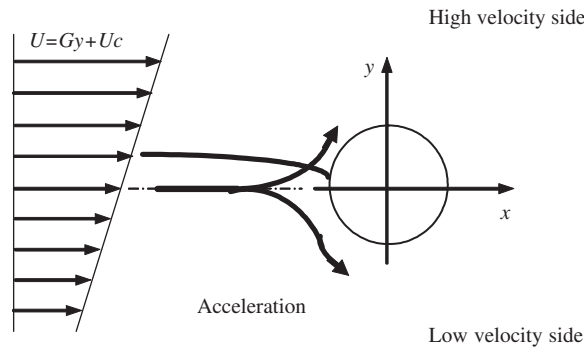Fig. 11. Comparison between pressure distributions in shear flow and uniform flow.

Fig. 12. Illustration of flow in shear flow.

pressure from the stagnation point to the minimum pressure point on the low velocity side. After that, the velocity shear function dominates and results in larger pressure on the low velocity side. The base pressure is determined by the interaction of the two separated shear layers, so that there is no significant difference between the two sides of the cylinder. It can also be seen from Fig. 10 that the separation point in the shear flow shifts downstream on the high velocity side, and moves upstream on the low velocity side, unlike that in uniform flow. With the increase in shear parameter, the shifts in separation point are more significant.

The aerodynamic forces acting on the cylinder can be calculated by integrating the pressure distribution around it. Compared to the pressure distribution in uniform flow (see Fig. 11), the pressure of the forebody in shear flow is obviously larger on the high velocity side and smaller on the low velocity side. This is due to the dislocation of the stagnation point. However, their total contribution to the drag is small because they cancel each other out to some extent. Meanwhile, base pressure recovers significantly with a contribution to drag decrease. Integration of the pressure around the cylinder results in a decreased drag coefficient in shear flow at subcritical Reynolds region. The velocity shear, rather than the dislocation of the stagnation point, contributes more to the drag decrease. Fig. 13(a) shows the reduction of drag coefficient with shear parameter. Reduction of drag in shear flow was noticed by Sumner and Akosile (2003), Kwon et al. (1992) and Hayashi and Yoshino (1990), but not by Adachi and Kato (1975). Deviations of the results between the present and cited studies are obvious in both shear and non-shear flows, possibly because of the differences of blockage ratio, aspect ratio and turbulence level. Meanwhile, a mean lift force, which does not occur in the uniform flow, exists due to the asymmetry of the pressure distribution mainly due to the dislocation of the stagnation point. Although the pressure is larger on the low velocity side within the region of $70° < |\theta| < 90°$ due to the velocity shear effect that creates a lift force from the low velocity side to the high velocity side, the pressure is larger on the high velocity side within the region of $|\theta| < 70°$ due to the dislocation of the stagnation point, which creates a lift force from the high velocity side to the low velocity side. Fig. 13(b) shows that the total lift force acts from the high velocity side to the low velocity side. This is because the contribution from the dislocation of stagnation point is larger. An increase of lift force with a direction from high velocity to low velocity side was reported also by Sumner and Akosile (2003), Kwon et al. (1992), Hayashi and Yoshino (1990) and Kato and Adachi (1976), shown in Fig. 13(b). Differences of blockage ratio, aspect ratio and turbulence level are considered to be the reason for the difference in decrease rate of lift force between present and cited studies. However, Tamura et al. (1980) investigated the variation of drag and lift forces with shear parameter numerically at Re = 40 and 80. They reported that the lift force increases with shear parameter, as in the present study, but the lift force was shown to act from the low velocity side to high velocity side. They explained this as the result of a smaller minimum pressure at $\theta = 90°$ on the high velocity side, which creates a lift force toward the high velocity side. The contribution of the dislocation of the stagnation point was not mentioned in their study. We think this was possibly because the Reynolds number was too small in their study and viscosity did not function as in the present study. Actually, a similar inconsistency in the lift force direction can also be found in the studies of the flow past a sphere in shear flows (Dandy and Dwyer, 1990; Kurose and Komori, 1996), perhaps also because of the Reynolds number dependence. The present study shows that the aerodynamic forces on a circular cylinder in shear flow are determined by the pressure distributions that are subject to the combined effect of velocity
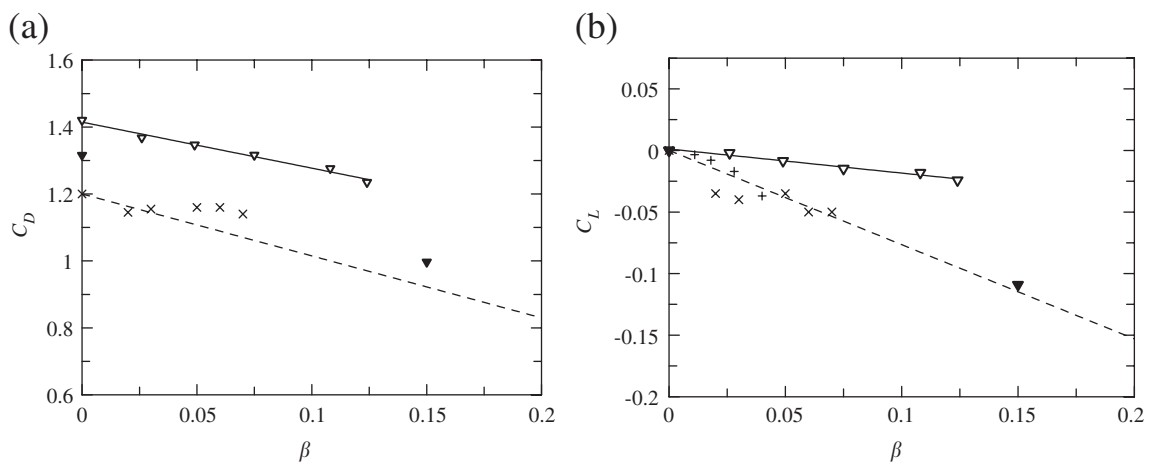

Fig. 13. Variations of drag force and lift force with shear parameter: - - -, Kwon et al. (1992), trend lines for reference only; other symbols, as in Figs. 4 and 7. (a) Drag, (b) lift.

shear and dislocation of stagnation point, which contribute in opposite senses to the lift force direction. Therefore, any factors that may influence the flow pattern, including Reynolds number, body shape and geometry, may change the individual contributions of these two flow features and lead to different aerodynamic forces in shear flow.

5. Conclusions

The effects of velocity shear on vortex shedding and aerodynamic forces on a cylinder with its axis normal to the plane of the shear profile were investigated experimentally in the subcritical Reynolds number range. Experiments were carried out in actively controlled multiple fan wind tunnels, which easily generate linear shear flow. The variations of Strouhal number, mean and fluctuating base pressure with shear parameter were examined to study the vortex shedding behavior. Variations of mean pressure distributions around a cylinder in shear flow were also investigated. Effects of dislocation of the stagnation point and the velocity shear on the pressure distributions were discussed. Variations of drag and lift forces acting on the cylinders with shear parameter and the physical mechanism for these variations were presented.

The Strouhal number was almost unchanged when the shear parameter was less than 0.27 at subcritical Reynolds number. The vortex shedding was suppressed in the shear flow. Large acceleration on the low velocity side occurred due to the dislocation of the stagnation point. The vortex was strengthened and weakened on the high and lower velocity sides, respectively, as it moved downstream. A very complicated vortex street was present in the far wake.

The base pressure increased with increasing shear parameter. The fluctuating component of base pressure decreased with increasing shear parameter. The separation point in the shear flow shifted downstream on the high velocity side and moved upstream on the low velocity side, unlike that in uniform flow. With increasing shear parameter, the shifts of separation point were more significant.

Velocity shear and dislocation of the stagnation point influenced the pressure distribution around the cylinder simultaneously, but with opposite effects. For the cylinder at $Re = 3.64 \times 10^4$, the drag force decreased with increasing shear parameter, mainly due to the effects of the velocity shear that caused recovery of the base pressure. A lift force occurred in the shear flow due to the asymmetry of pressure distribution around the cylinder, and acted from the high velocity side to the low velocity side. Dislocation of the stagnation points contributed more to the lift force than the velocity shear. When the aerodynamics of a bluff body in shear flow are under investigation, Reynolds number, body shape and geometry must be taken into consideration, because they may influence the flow pattern and consequently the individual contributions of velocity shear and dislocation of stagnation point to pressure distribution, and result in different aerodynamic forces in shear flow.

References

Adachi, T., Kato, E., 1975. Study on the flow about a circular cylinder in shear flow. Transactions of the Japan Society for Aeronautical and Space Sciences 256, 45–53.

Basu, R.I., 1986. Aerodynamic forces on structures of circular cross-section, Part 2, the influence of turbulence and three-dimensional effects. Journal of Wind Engineering and Industrial Aerodynamics 24, 33–59.

Bearman, P.W., 1965. Investigation of the flow behind a two-dimensional model with a blunt trailing edge and fitted with splitter plates. Journal of Fluid Mechanics 21, 241–257.

Cao, S., Hirano, K., Ozono, S., Wakasugi, Y., 2000. Vortex shedding for a circular cylinder placed in strong shear flow. Journal of Wind Engineering 85, 53–62 (in Japanese).

Cao, S., et al., 2001. An actively controlled wind tunnel and its application to the reproduction of the atmospheric boundary layer. Boundary Layer Meteorology 101 (1), 61–76.

Dandy, D.S., Dwyer, H.A., 1990. A sphere in shear flow at finite Reynolds numbers, effect of shear on particle lift, drag and heat transfer. Journal of Fluid Mechanics 216, 381–410.

Hayashi, T., Yoshino, F., 1990. On the evaluation of the aerodynamic forces acting on a circular cylinder in a uniform shear flow. Transactions of the Japan Society for Mechanical Engineering 56 (552), 31–36.

Kato, E., Adachi, T., 1976. An effect of the velocity gradient of main flow on the vortex shedding from a circular cylinder. Transactions of the Japan Society for Aeronautical and Space Sciences 270, 25–33.

Kiya, M., Arie, M., Furukawa, M., 1979. Formation of the vortex street in shear flow. Transactions of the Japan Society for Mechanical Engineering 45 (389), 1–10.

Kiya, M., Tamura, H., Arie, M., 1980. Vortex shedding from a circular cylinder in moderate-Reynolds-number shear flow. Journal of Fluid Mechanics 141, 721–735.

Kurose, R., Komori, S., 1996. Evaluation of the fluid force on a sphere rotating in shear flow. Transactions of the Japan Society for Mechanical Engineering 62 (599), 10–17.

Kwon, T.S., Sung, H.J., Hyun, J.M., 1992. Experimental investigation of uniform shear flow past a circular cylinder. ASME Journal of Fluids Engineering 114, 457–460.

Maskell, E.C., 1963. A theory on the blockage effects on bluff bodies and stalled wings in a closed wind tunnel. Aeronautical Research Council, No. 3400.

Ozono, S., 1999. Flow control of vortex shedding by a short splitter plate asymmetrically arranged downstream of a circular cylinder. Physics of Fluids 11, 2928–2934.

Ozono, S., Aota, N., Ohya, Y., 1997. Stably stratified flow around a horizontal rectangular cylinder in a channel of finite depth. Journal of Wind Engineering and Industrial Aerodynamics 67/68, 103–116.

Sasaki, K., Hirano, H., 1978. Effects of flow depth on the flow around a circular cylinder near critical Reynolds number. Transactions of the Japan Society for Mechanical Engineering 40 (385), 3044–3051.

Sumner, D., Akosile, O.O., 2003. On uniform planar shear flow around a circular cylinder at subcritical Reynolds number. Journal of Fluids and Structures 13, 309–338.

Tamura, H., Kiya, M., Arie, M., 1980. Numerical simulation of the shear flow past a circular cylinder. Transactions of the Japan Society for Mechanical Engineering 46 (404), 555–564.

Tamura, H., Kiya, M., Arie, M., Saito, T., 1981. Vortex shedding from a circular cylinder in linear shear flow. Transactions of the Japan Society for Mechanical Engineering 47 (414), 245–250.

West, G.S., Apelt, C.J., 1982. The effects of blockage and aspect ratio on the mean flow past a cylinder with Reynolds numbers between 10^4 and 10^5. Journal of Fluid Mechanics 114, 361–377.

Woo, H.G., Cermak, J.E., Peterka, J.A., 1989. Secondary flows and vortex formation around a circular cylinder in constant shear flow. Journal of Fluid Mechanics 204, 523–542.